Journal of Zhejiang University SCIENCE
ISSN 1009-3095
http://www.zju.edu.cn/jzus
E-mail: jzus@zju.edu.cn

A novel fabrication of meso-porous silica film by sol-gol of TEOS*

YIN Ming-zhi (殷明志)†, YAO Xi (姚 熹), ZHANG Liang-ying (张良莹)

(*Electronic Materials Research Laboratory, Xi'an Jiaotong University, Xi'an 710049, China*)

†E-mail: ymingzhi@nwpu.edu.cn

Received May 7, 2003; revision accepted Sept. 19, 2003

Abstract: A homogeneous crack-free nano- or meso-porous silica films on silicon was fabricated by colloidal silica sol derived by hydrolyzing tetraethyl orthosilicate (TEOS) catalyzing with $(C_4H_9)_4N^+OH^-$ in water medium. The solution with ratio of H_2O/TEOS≥15, R_4N^+ and glycerol as templates, combining with the hydrolyzed intermediate, controlled the silica aggregating; the templated silica film with heterostructure was developed into homogeneous nano-porous then meso-porous silica films after being annealed from 750 °C to 850 °C; the formation mechanism of the porous silica films was discussed; morphologies of the silica films were characterized. The refractive indexes of the porous silica films were 1.256−1.458, the thermal conductivity < 0.7 W/m/K. The fabricating procedure and the sequence had not been reported before.

Key words: Tetraethyl orthosilicate (TEOS), Sol-gel technique, Porous silica film, Thermal conductivity
Document code: A **CLC number:** TB321

INDRODUCTION

Meso-porous silica films with an excellent heat-insulating property and the relatively low dielectric value play particularly important role in electronic and magnetic devices (Moon *et al.*, 1997), etc.; those with pore sizes of 5 nm to 50 nm are also of interest for applications in photonics, optoelectronics, lightweight structural material thermal insulation, optical coating (Moon *et al.*, 1997; Husing and Schulert, 1998; Davis, 2002). Their special network structure is used in sound detector (Husing and Schubert, 1998); their excellent insulating property and its near perfect interface on silicon play a key role in the success of very large scale integrated (VLSI) devices (Moon *et al.*, 1997) due to the size and shape of selected porous silica films, they can also be used as adsorbents, scaffolds for composite material synthesis, in separation technology (Avelino, 1997), molecular engineering, and biological engineering, etc. (Gill and Ballesteros, 1998). Currently used silica films with high refractive indices can thereby be replaced by porous silica films so that more light can reach the active surface because of the lower scattering losses and the efficiency of the solar cell is thus increased. In view of the applications mentioned above, nano- and meso-porous silica films with uniform pore diameter of 50–300 nm have attracted great attention in the aspect of their fabrications; and the extensive efforts have been made in this area (Lu *et al.*, 1997; Zhao *et al.*, 1998; Johnson *et al.*, 1999). However, the preparing procedures were broadly focused on the templated-surfactant micellar effect. Here we fabricated nano- and meso-porous silica films via sol-gel process of tetraethyl orthosilicate (TEOS) catalyzed by $R_4N^+OH^-$ in aqueous medium. The technique yields silica sol precursor composed of individual silica particles of controllable shape and

* Project (No. 2002CB613305) supported by the National Basic Research Program (973) of China

size, and the silica films with porous diameters of 100−200 nm (nano- to meso-porous). The morphologies and physical properties of the porous silica films were characterized.

EXPERIMENTS

The colloidal silica sol used was prepared as follows:

(1) After 15 ml 2.4 mol/L $AgNO_3$ was gradually added into 50 ml 0.925 mol/L NaOH solution under stirring, the precipitated Ag_2O was filtered from the solution with glass funnel.

(2) A solution, formed by dissolved 9.72 g $N(C_4H_9)_4Cl$ (0.035 moles) in 15 ml absolute C_2H_5OH, reacted the precipitated Ag_2O and formed $N^+(C_4H_9)_4\,OH^-$ solution after the AgCl was filtered with glass funnel.

(3) 20.8 g TEOS (0.10 moles) was allowed to react with the $(C_4H_9)_4N^+OH^-$ solution under stirring for 60 min, and formed a homogeneous silica colloidal sol which was neutralized by addition of 2–4 ml $CH_3COOC_2H_5$ hydrolyzing under stirring for 60 min, and polymerized by addition of 10–15 ml 5 wt % PVA water solution, and finally filtered with slow filter and became the silica sol precursor.

(4) The silica sol precursor was dropped on fixed Si wafer; then was spun-coating at 3000–3500 rev/min for 20 seconds in 100-class ultra-clear room. The coated silica films were thermal treated at 350 ºC for 30 min in furnace. Recycling of the operations was continued until the desired thickness was obtained finally, the silica films were annealed at the desired temperature for 30 min.

DTA DGA of the silica sol precursor were conducted by Dupont TA-2000 thermal analysis instrument (TA Instrument Inc. USA); grain distribution of the silica sol was characterized by BI-90 Laser scatter (Brookhaven Instrument Co., He-Ne Laser); surface morphologies of the porous silica films were observed by scanning electron microscopy (SEM) (Hitachi S-2700); refractive indexes of the porous silica films were measured by ellipsometer (Mizojiri Optical Co Ltd DVA-36LD) at its most shallow incident angle of 30º; pore distributions of the porous silica films were obtained by calculation of the refractive indexes; the thermal parameters of the films were measured with 3ω method.

RESULTS AND DISCUSSIONS

Chemical mechanism of the sol-gel process of $Si(OC_2H_5)_4$

One of the interesting topics in material investigation is synthesis of hetero-structural materials in which the networks can be organized into some architecture with unique shape. The nano- and meso-porous silica films can be obtained by careful control of the synthesis conditions. Designing and fabricating porous silica films with defined morphologies must begin from preparation of the silica sol precursor. Under the experimental conditions, the formation of the organic base $(C_4H_9)_4N^+OH^-$ solution is as follows:

$$2(C_4H_9)_4N^+Cl^-+Ag_2O+2C_2H_5OH \rightarrow 2(C_4H_9)_4N^+OC_2H_5^-+H_2O+2AgCl(s)\downarrow \quad (1)$$

AgCl and excess Ag_2O are removed by filtering with glass funnel; the solution is diluted with water as the sol-gel medium of TEOS,

$$(C_4H_9)_4N^+OC_2H_5^-+H_2O=(C_4H_9)_4N^+OH^-+HOC_2H_5 \quad (2)$$

Under the strong basic conditions,

$$(OC_2H_5)_3SiOC_2H_5+H_2O \xrightarrow{OH^-} (OC_2H_5)_3SiOH+HOC_2H_5 \quad (3)$$

$$(OC_2H_5)_3SiOH+(x-1)H_2O \rightarrow Si(OC_2H_5)_{4-x}(OH)_x+(x-1)HOC_2H_5 \quad (4)$$

The hydrolyzing process of TEOS is a nucleophilic reaction of OH^- on the silicon atom of TEOS, following a relatively slow removal of first OC_2H_5 which is much faster than hydrolysis of the $Si(OC_2H_5)_{4-x}\,(OH)_x$; the active products are easily polymerized into $Si_xO_y(OH)_z$ or undergone silica particle precipitation by interaction of HO-Si group

by H-band,

$$(OC_2H_5)_3SiO^-+(OC_2H_5)_3Si\text{-}OH \rightarrow (OC_2H_5)_3Si\text{-}O\text{-}Si(OC_2H_5)_3(OH)^- \rightarrow (OC_2H_5)_3Si\text{-}O\text{-}Si(OC_2H_5)_3+OH^- \quad (5)$$

$$Si(OH)_5^-+Si(OH)_4\rightarrow(OH)_3Si\text{-}O\text{-}Si(OH)_3 \quad \text{or}$$

$$\rightarrow(OH)_2\overset{O}{\diagup\diagdown}Si\text{-}O\text{-}Si(OH)_2+H_2O \quad (6)$$

$$n(OH)_2Si\text{-}(OH)_2\text{-}Si(OH)_2\rightarrow Si_xO_y(OH)_z+mH_2O \quad (7)$$

The active $Si_xO_y(OH)_z$ either participates in growth of silica particles or forms new nuclear of silica particles based on the reactive conditions,

$$Si_xO_y(OH)_z \begin{cases} \nearrow \text{Being deposited on the surface of the silica particles} \\ \searrow \text{Forming new silica particles} \end{cases} \quad (8)$$

If concentration of the $Si_xO_y(OH)_z$ exceeds some value, silica particles are grown through aggregation of the $Si_xO_y(OH)_z$, and formed un-homogeneous silica particles, even a precipitated silica; if the growth of silica particles is limited, new silica particles are formed. With $C_3H_5(OH)_3$ in the sol-gel medium, $Si_xO_y(OH)_z$ is in the form of a $Si_xO_y(OH)_z$ wapped up in $C_3H_5(OH)_3$, which decreases or eliminates aggregating of the Si_xO_y $(OH)_z$, and new silica particles are formed rapidly in condensed, smaller, uniform form; furthermore, the higher pH makes the silica particles charged negatively, and re-dissolved, which also prevents aggregation of silica particles. In order to formation of the colloidal silica sol film, the pH is neutralized by hydrolyzing of $CH_3COOC_2H_5$ homogeneously. The silica grain distribution of the silica sol precursor is shown in Fig.1.

The cumulative undersize distribution is 10% for diameter below 16 nm, about 80% for diameter 16 to 73 nm, and 10% for diameter over 73 nm.

So, silica sol precursor with uniformly granular nm silica particles can be obtained by controlling the sol-gel conditions.

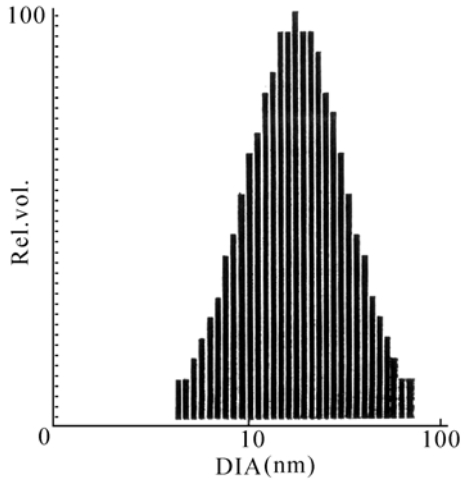

Fig.1 Silica grain distribution of colloidal silica sol

Template effect

The template effects can: (1) Control growth of silica particles of colloidal silica sol; (2) Control existence state of the silica. In addition to the effects, nonionic polymeric binder poly (vinyl-alcohol) PVA produces colloidal silica sol with polymeric structure. But PVA ability to absorb many silica particles simultaneously leads to "bridging", or promotes undesirable bridging flocculation polymers. The $C_3H_5(OH)_3$ can reduce the adsorbing drastically by occupying the most reactive adsorption sites of the silica.

Cracking of the silica films can also be controlled through the templates. The templates are trapped within silica films and form a modulated structure; relaxation of the heterostructure can decrease thermal stress of the silica film when it is being annealed. Furthermore, the templates migrate to the silica film surface with flow of solvent within the silica and accumulate as solvent evaporated; the un-uniform distribution of the templates can lead to an elastic surface, which can prevent the silica film from being cracked.

Porous evolution of the silica film

Fig.2 shows photographs of the silica film after it was annealed at different temperatures; the gel silica film contains silica and organic templates. After being annealed at 550 ºC for 30 min, the tem-

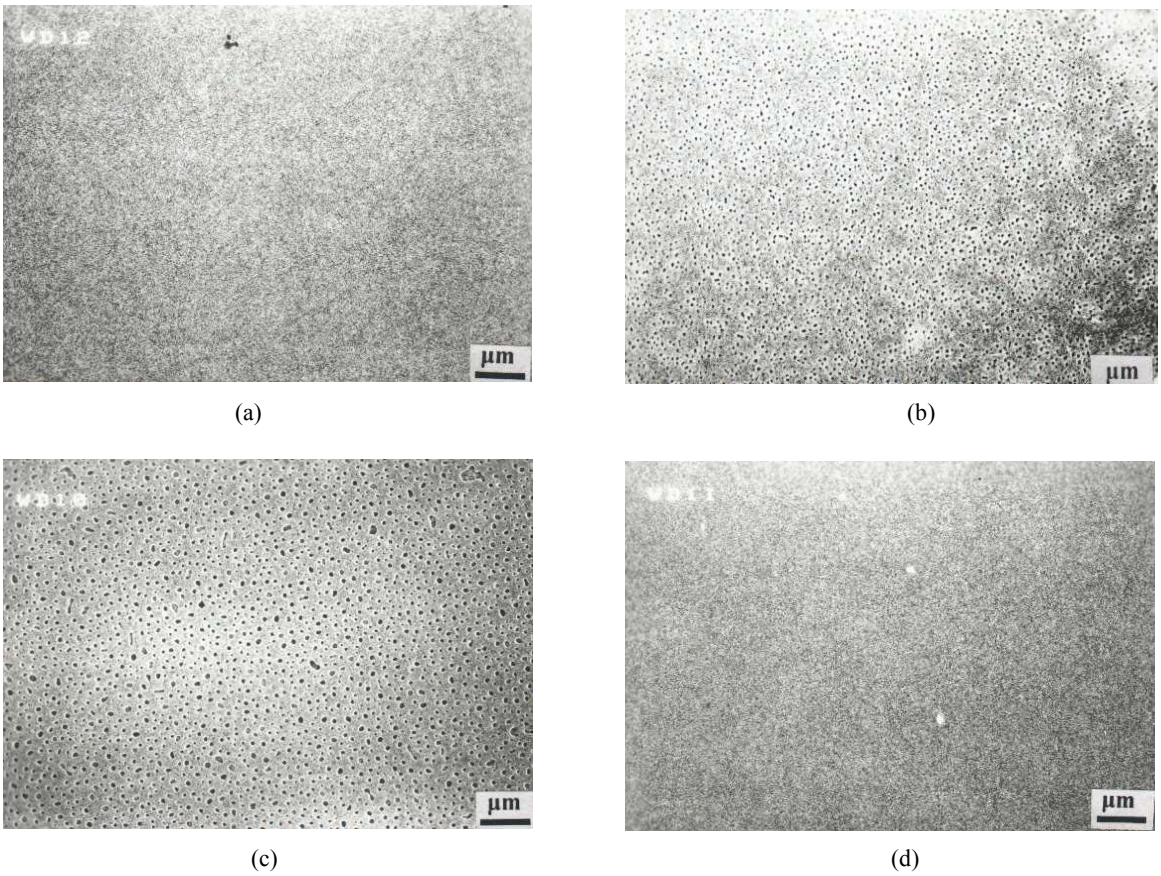

(a) (b)

(c) (d)

Fig.2 SEM evolution process of porous silica film
(a) 550 °C/30 min; (b) 750 °C/30 min; (c) 850 °C/30 min; (d) 950 °C/30 min

plates are burned out and Si-OH is polymerized, the silica film appears compacted; after being annealed at 750 °C for 30 min, the silica film appears nano-porous due to silica plastic strain; the nano-porous structure is reformed into a meso-porous structure after being annealed 850 °C; the mean pore sizes are 100 nm to 200 nm. Furthermore, silica particles composing the film were developed into joined necks; silica walls are as hard as granular silica due to the basic thermal strain from water and OH^-, which reinforces the silica film with much higher porosity. When being annealed at 950 °C for 30 min, the silica film appears compacted.

In gel silica film made by aggregated silica particles with glycerol and PVA, after the templates burn out and the aggregated silica particles polymerize, more pores are left within the silica films. The aggregated silica particle network prevents collapsing of the porous structure when the silica film is being annealed.

Refractive indexes of silica film

Increasing of the refractive index of the silica film is attributed to dehydration and polymerization of the silica caused by the annealing process; the plastic strain of silica film at higher annealing temperature increases porosity. Polymerizing of Si-OH within the silica accompanies the silica film shrinkage. The relationship of porosity and refractive index of the silica film can be expressed as:

$$(n^2-1)/(n_c^2-1)=(1-p)/100 \quad (9)$$

where n and n_c are refractive indexes of porous film and their nonporous film respectively, and p is the porosity. The value of refractive index of nonpor-

ous silica bulk glass is 1.458. Table 1 lists the refractive indexes of the silica film characterized by ellipsometer using an average wavelength (632.8 nm).

Relative densities (Parrill, 1994)

$$\rho_r = K(n^2-1)/(n^2+2) \quad (10)$$

where K is material constant，and ρ_r is the relative density of the porous silica film, it is compared with that of the silica film after being annealed at 1150 °C/30 min. For the porous silica film, ρ_r can be calculated with:

$$\rho_r = N_r(n^2-1)/(n^2+2) \quad (11)$$

$$N_r = [(1.58)^2+2]/[(1.58)^2-1] \quad (12)$$

The refractive index of the silica film is increased after annealing the film from 450 °C to 850 °C.

Table 1 Refractive indexes of silica film characterized by ellipsometer using average wavelength (632.8 nm)

Film	Annealing (°C/min)	Refractive index	Porosity (%)	Dielectric constant $K=n^2$ [a]	Relative density ρ_r
Silica film	550/30	1.256	48.7	1.578	0.592
	650/30	1.237	52.9	1.530	0.550
	750/30	1.316	35.0	1.732	0.719
	850/30	1.420	9.70	2.016	0.926
	950/30	1.456	0.53	2.120	0.996
Fused SiO_2	1150/30	1.458[b]	0.00	2.126	1.000

[a](Moon *et al*., 1997); [b](Parrill, 1994)

Thermal conductivity of the porous silica film

The observed striking thickness dependence of the porous silica film thermal conductivity in the investigations was interpreted using approach proposed by Lambropoulos *et al*.(1989). Substantial thermal resistance of silica film was developed at the film/substrate interface and within the silica films. The interfacial thermal resistance dominated the thermal resistance of the film. Lambropoulos *et al.*(1989) argued that the presence of a large interfacial resistance implies that temperature was virtually discontinuous across the interface. Combining the linear function of heat flux across the silica film, he established the following relationship:

$$K(d)=K_1 d/(K_2 K_1+d) \quad (13)$$

In Eq.(13), $K(d)$ is the experimentally determined and is the thickness-dependent apparent thermal conductivity of the thin silica film; K_1 is the intrinsic thermal conductivity of the silica film; d is the thickness of the silica film and K_2 is the interfacial thermal resistance.

Thermal conductivity measurements of the silica film was performed using a 3ω method (Tsuneyuki *et al.*, 2002).

The silica film was prepared on about 0.5 mm thick Si substrate by using the sol-gel process and different techniques. i.e. such as thermal oxidation, CVD, and sputtering. The conditions of the processes were those conventionally used for fabricating semiconductor devices. The Al or Au metal line was produced on the sample surfaces with the microlithographic method used for producing electronic microcircuits. The metal lines used in this study were 8 μm wide, 1.4 mm long, and about 0.3 μm thick. The width and length of the metal line were measured using a microscope equipped with a calibrated scale viewer. The measurements were performed in a vacuum (about 10^{-5} Torr). The results are listed in Table 2.

The thermal conductivity of the meso-porous silica film was less than intrinsic thermal conductivity of the crystal silica $K^{SiO_2}_{int}$ (1.47 w/m/k). For silica films less than 1 μm, the thermal conductivity is less than that of the bulk silica over the temperature. The relation of the thermal conductivity with thickness is as shown in Fig.3.

Table 2 Thermal parameters of the silica films measured with 3ω method

Parameters	Meso-porous silica film	SiO_2 film		
		Thermal oxidation	CVD	Magnetron sputtering
Density (g/cm^3)	0.588–0.759	0.973	0.909	0.990
Porosity (%)	51.1–32.1	2.7	9.1	1.0
Pore diameter (nm)	100			
Thermal conductivity (W/m/K)	<0.7	1.38	1.00	1.1

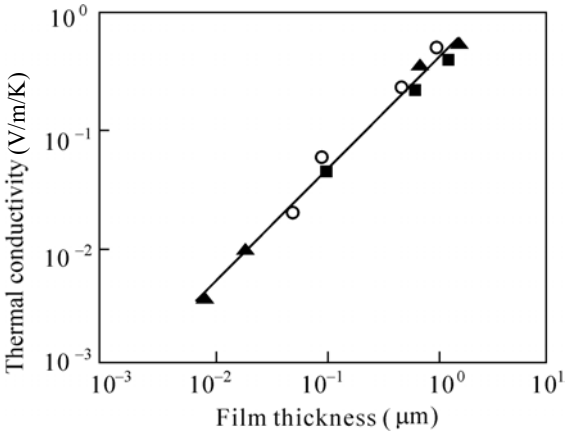

Fig.3 The average apparent thermal conductivity of silica films plotted as a function of the thickness (Griffin Land Brotzen, 1994)

The solid line (—) is the least-squares curve fit conforming to Eq.(13); ▲ thermally grown silica film; ■ CVD silica film; ○ silica film

CONCLUSION

1. A new method for preparing crack-free homogeneous nano- or meso-porous silica film on silicon is developed. The silica film is fabricated by colloidal silica sol derived by hydrolyzing tetraethyethyl orthosilicate (TEOS) catalyzing with $R_4N^+OH^-$ in glycerol water.

2. Glycerol can control aggregating of the hydrolyzing intermediates $Si_xO_y(OH)_z$ while Poly (vinyl-alcohol) (PVA) produces the colloidal silica sol with polymeric structure.

3. The templated silica film with a hetero-structure can be developed into a homogeneous nano-porous even meso-porous silica film after being annealed.

References

Avelino, C., 1997. From micro-porous to meso-porous molecular sieve materials and their use in catalyst. *Chem. Rev.*, **97**:2373-2381.

Davis, M.E., 2002. Ordered porous materials for emerging applications. *Nature*, **417**:813-816.

Gill, I., Ballesteros, A., 1998. Encapsulation of biologicals within silicate, siloxane, and hybrid sol-gel polymers: An efficient and generic approach. *J. Am. Chem. Soc.*, **120**:8587-8592.

Griffin, A.J.Jr, Brotzen, F.R., 1994. Effect of thickness on the transverse thermal conductivity of thin dielectric films. *J. Appl. Phys.*, **75**(8):3761-6737.

Husing, N., Schubert, U., 1998. Aerogel Airy Material: structure, chemistry, structure, and properties. *Angew Chem. Int. Ed.*, **37**:22-29.

Johnson, S.A., Ollivier, P.J., Mallouk, T.E., 1999. Ordered meso-porous polymers of tunable pore size from colloidal silica templates. *Science*, **283**:963-966.

Lambropoulos, J.C., Jolly, M.R., Amsden, C.A., Gilman, S.E., Sinicropi, M.J. Diakomihalis, D., Jacobs, S.D., 1989. Thermal conductivity of dielectric thin films. *J. Appl. Phys.*, **66**(9):4230-4236.

Lu, Y.F., Qangull, R., Drewien, C.A., Anderson, M.T., Brinker, C.J., Gong, W., Guo, Y.X., Soyez, H., Dunn, B., Michael, H.H., Jeffrey, Z., 1997. Continuous formation of supported cubic and hexagonal meso-porous films by sol-gel dip-coating. *Nature*, **389**:364-367.

Moon, H.J., Hyung, H.P., Dong, J.K., Sang, H.H., Choi, S.Y., Paik, J.T., 1997. SiO_2 aerogel film as a novel intermetal dielectric. *J. Appl. Phys.*, **82**(3):1299-1305.

Parrill, T.M., 1994. Heat treatment of spun-on acid-catalyzed sol-gel silica films. *J. Mater. Res.*, **9**:723-728.

Tsuneyuki, Y., Nagai, N., Katayama, S., Todoki, M., 2002. Measurement of thermal conductivity of silicon dioxide thin films using a 3ω method. *J. Appl. Phys.*, **91** (12): 9772-9779.

Zhao, D.Y., Feng, J.G., Huo, Q.S., Melosh, N., Fredrickson, G.H., Chmelka, B.F., Stucky, G.D., Copolymer, T., 1998. Syntheses of meso-porous silica with periodic 50 to 300 angstrompores. *Science*, **279**: 548-551.